

Direct formation of nitrogen-vacancy centers in nitrogen doped diamond along the trajectories of swift heavy ions

Russell E. Lake,^{1,2} Arun Persaud,¹ Casey Christian,¹ Edward S. Barnard,³ Emory M. Chan,³ Marilena Tomut,^{4,5} Christina Trautmann,^{4,6} and Thomas Schenkel¹

¹*Accelerator Technology & Applied Physics, Lawrence Berkeley National Laboratory, 1 Cyclotron Road, Berkeley, CA 94720, USA*

²*QCD Labs, COMP Centre of Excellence, Department of Applied Physics, Aalto University, P.O. Box 13500, FI-00076 Aalto, Finland*

³*The Molecular Foundry, Lawrence Berkeley National Laboratory, 1 Cyclotron Road, Berkeley, CA 94720, USA*

⁴*GSI Helmholtz Center for Heavy Ion Research, 64291 Darmstadt, Germany*

⁵*Institute of Materials Physics, WWU Münster, Wilhelm-Klemm-Straße 10, 48149 Münster, Germany*

⁶*Technical University of Darmstadt, 64287 Darmstadt, Germany*

(Dated: 26 June 2022)

We report depth-resolved photoluminescence measurements of nitrogen-vacancy (NV^-) centers formed along the tracks of swift heavy ions in type Ib synthetic single crystal diamonds that had been doped with 100 ppm nitrogen during crystal growth. Analysis of the spectra shows that NV^- centers are formed preferentially within regions where electronic stopping processes dominate and not at the end of the ion range where elastic collisions lead to formation of vacancies and defects. Thermal annealing further increases NV yields after irradiation with SHI preferentially in regions with high vacancy densities. NV centers formed along the tracks of single swift heavy ions can be isolated with lift-out techniques for explorations of color center qubits in quasi 1D registers with average qubit spacing of a few nm and of order 100 color centers per micron along 10 to 30 micron long percolation chains.

I. INTRODUCTION

The negatively charged nitrogen-vacancy (NV^-) defect center in diamond has gained much attention for applications in quantum optics due to its long coherence time at room temperature and its great potential for quantum sensing and quantum communication.^{1–3} Reliable formation of color centers with long spin coherence times and the placement of color centers into quantum registers are a major challenge for applications. This is in part due to the fact that our understanding of the microscopic formation mechanisms of NV centers has remained incomplete. In particular, density functional theory apparently contradicts some experimental results.⁴ Studies of color center formation processes under a series of experimental conditions can help support advances towards deterministic formation of high quality color centers.¹

From the perspective of quantum device fabrication, it will be useful to place single color centers into precise locations of a sample. This calls for modes of fabrication with high spatial resolution. Here, we report on the formation of color centers in diamond along the trajectories of swift heavy ions. Swift heavy ions (SHI), such as gold ions at 1.1 GeV, transverse solids along near straight lines over distances of tens of microns with high probability. We report that NV centers form in the interaction of SHI with nitrogen doped diamond directly, without any thermal annealing. In many earlier studies, energetic ions and electrons have been used to first form vacancies and then NV-centers in diamonds during a consecutive thermal annealing step.⁵ Hence, we observe an efficient one-

step process for local color center formation with alignment of color centers along the trajectory of each SHI. In an earlier study, we had observed the formation of NV centers following irradiation of diamonds with SHI where the diamonds had been implanted with nitrogen ions over a depth of about 100 nm near the diamond surface.⁶ The motivation for our current study was two-fold. In addition to the development of new fabrication tools for diamond-based quantum-photonic devices,⁷ we also seek to understand the role of intense electronic excitations on color center formation within the non-equilibrium process of track formation.⁸ Swift heavy ion tracks in diamond have recently been treated with computational methods.^{9–11} Efforts to engineer non-Poissonian spatial distributions of color centers in diamond have included, among others, the use of He ions,^{12–14} 60 keV N ions,¹⁵ highly charged Ar ions,¹⁶ and beams of energetic electrons in pre-implanted diamond.¹⁷ NV center yields of up to about 50% have been reported,¹⁸ but much lower yields are common.¹⁹ Recently progress has been reported on achieving a higher NV center yield using ion implantation and local doping of diamonds.²⁰ While higher color center yields have been reported, underlying mechanisms of competing color center processes remain to be disentangled and formation of spin-photon qubit registers with (sub-)10 nm resolution as required for nearest neighbor coupled qubits with magnetic dipolar interaction remain a challenge. In this article we report on the depth distribution of NV^- centers formed by the irradiation of swift heavy ions prior to and after an additional thermal annealing step. We observe NV- creation in regions of high electronic stopping, as opposed to regions

where vacancy defects are created by nuclear collisions.⁴ We briefly outline integration of 1D color center chains for spin-photon qubit explorations.

II. EXPERIMENTAL SETUP

The samples studied in this work were type Ib diamonds (Element Six) with approximately 100 ppm N present from chemical vapor deposition growth. During irradiation with swift heavy ions the sample was masked by a thick metallic grid with millimeter-sized openings to allow for both irradiated and non-irradiated regions to be measured at the same time. Irradiations were carried out at the Helmholtzzentrum für Schwerionenforschung (GSI) with 1.1 GeV ^{197}Au ions with a fluence of 1×10^{12} ions/cm² using an ion beam flux of 6×10^9 ions/cm²/s. Gold ions at these energies have a range of 34 μm in diamond. After irradiation, the mask was removed and contrast between the irradiated and non-irradiated regions is visible by eye (Fig. 1c), where the darker regions of the sample were irradiated and the lighter regions were masked.

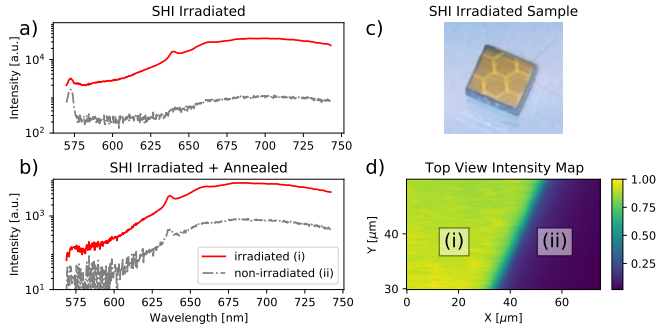


FIG. 1. Photoluminescence spectra of SHI irradiated diamond. The plots a) and b) show spectra from the SHI irradiated and later annealed samples. A photograph of the sample is shown in c) where the lighter regions are pristine and dark regions are irradiated. In d) a normalized count rate intensity map at fixed depth shows contrast between irradiated (i) and pristine (ii) regions of the irradiated and annealed sample.

We performed room temperature photoluminescence (PL) measurements across boundaries of the masked and irradiated regions. These measurements were performed with a custom built confocal PL setup designed for spatially resolved three dimensional maps of optically active defects in semiconductors with a similar experimental setup to Ref. 21. The sample was mounted with adhesive tape on a glass slide and placed on a piezo-nanopositioning sample stage. Control experiments on an annealed reference sample (1 ppm N) demonstrated that using this apparatus we can collect PL signals from the NV^- defects at depths of $>60 \mu\text{m}$, see Fig. 3d. Using the depth-resolved one-photon excitation-collection scheme²¹ photoluminescence was collected through a pinhole and into detection optics. For spectral mea-

surements we used an Acton 2300i spectrometer with 150 groves/mm grating and an Andor iXon electron-multiplied CCD. The excitation wavelength was 532 nm.

Initial measurements were performed after irradiating, and before annealing the sample, and are shown in Fig. 1a. PL spectra are measured within the irradiated (red line) and masked (gray line) regions. The intensity of the PL is enhanced in the regions that were irradiated by the ions. Qualitatively similar spectra are observed after annealing the sample in high vacuum at 800 °C for one hour in Fig. 1b. The difference in PL intensity between irradiated and non-irradiated areas can also be clearly seen in the contrast of Fig. 1d which shows a x - y map of the sample and the color represents the integrated measured PL spectra (normalized). The intensity of the PL spectra is measured in units of total photon counts per second within the wavelength span from 570 nm to 740 nm and is at least a factor of ten higher in the irradiated region compared to the non-irradiated region. We track the depth dependence of the spectral feature at $\lambda = 637 \text{ nm}$ associated with the NV^- centers using the experimental setup shown schematically in Fig 2. In

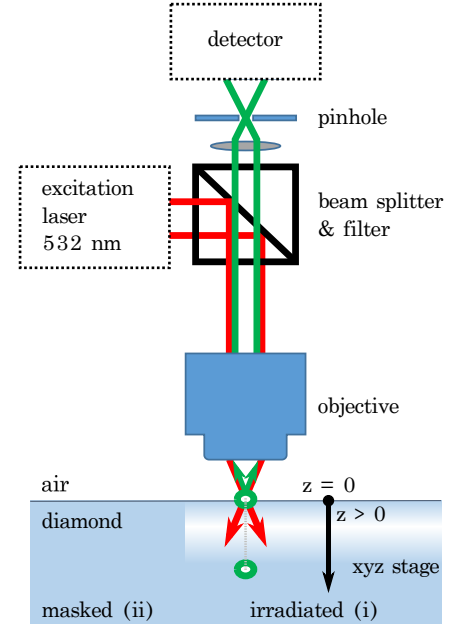


FIG. 2. Experimental schematic for three dimensional photoluminescence measurements

particular, we move the x - y - z sample stage while keeping the excitation laser focus position constant. We can thus scan the sample stage position to collect PL signal from a three dimensional volume within the sample.

To locate the stage position where the laser focuses on the surface, we add a filter to remove the PL contribution and record only the z -dependent reflection signal. The stage position at maximum reflection is identified as the surface position $z = 0$ and used to calibrate the z axis in Fig. 3.

As the stage moves toward the objective and the fo-

cus spot moves deeper into the sample, we record the PL spectrum for each location for 100ms. To convert from the stage position coordinate to the actual depth we optically excite in the diamond, we use the relation $z = n z_{\text{stage}}$, where n is the index of refraction in diamond $n = 2.4$. Although the stage has nanometer resolution, the depth resolution is given by light excitation and collection volumes which are stretched due to the high index of refraction of diamond. Using Eq. 1 from Ref. 22 we find that in our measurements (using $100\times$ lens, $\text{NA}=0.95$) the resolution scales proportionally to $4.6z_{\text{stage}}$ as we go deeper in the sample.

III. RESULTS

To analyze the data, we average the spatial regions to achieve better signal-to-noise spectra for the irradiated versus non-irradiated region (Fig. 1) or integrate just the NV peak at $\lambda = 637$ nm from 630 nm to 645 nm and the lateral spacial dimension to obtain the depth distribution of the NV centers as shown in Fig. 3.

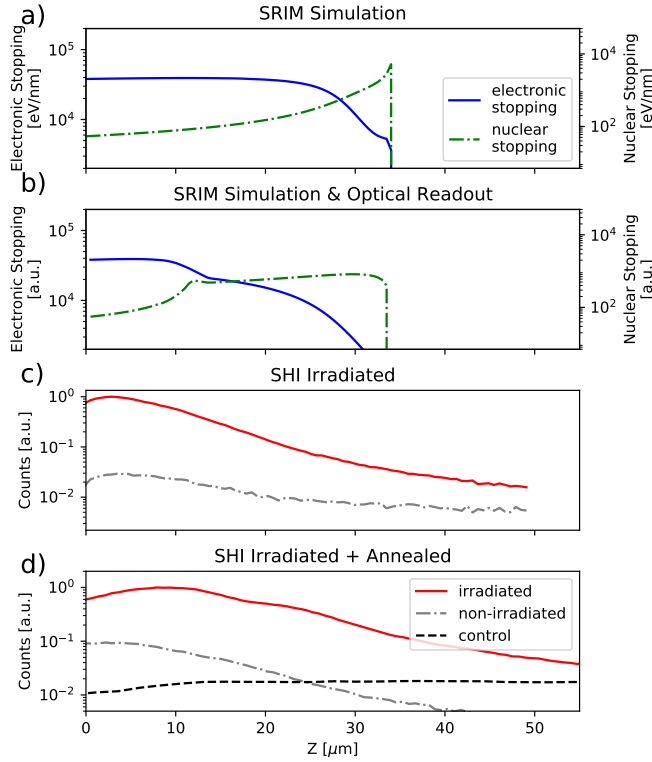


FIG. 3. a) SRIM simulation of 1.1 GeV Au ions into diamond showing contributions of the electronic and nuclear stopping processes along the ion paths. b) SRIM data convoluted with depth depended probe volume. c) depth profiles of the NV^- peak for the SHI-irradiated sample. d) depth profiles of the NV^- peak after annealing the sample combined with a measurement from a control sample with a uniform NV^- distribution.

Figure 3 displays the the depth profile of the inte-

grated PL around the NV line for the areas irradiated to SHI radiation (red), and the non-irradiated control regions (gray). Data from each panel are normalized to the maximum intensity measured in the irradiated region. In Figure 3a the results from an Stopping Ranges in Matter (SRIM)²³ are shown. In Figure 3b, we assume that NV centers are produced exclusively by either electronic or nuclear stopping and calculate the expected response by folding the simulated data from panel a) with the estimated probe volume. For the SHI irradiated sample in Fig. 3c we observe an increase in intensity within the irradiated region between the surface and a depth of approximately $5\mu\text{m}$ followed by a drop in intensity. The non-irradiated region of the sample shows a much weaker signal with a similar profile (possible due to light scattering). After the sample was annealed, we observe a similar characteristic profile with an additional shoulder at a larger depth. The anneal also activates NV center in the non-irradiated regions, although at a much lower intensity level.

IV. DISCUSSION

Using a diamond with a uniform distribution of nitrogen, we observe that NV centers are created by SHIs. The observed depth profile agrees well with the profile of the electronic stopping once we take the changes in probed volume into account. We also observe that SHI do not create NV centers at the end-of-range peak of nuclear stopping of the SHIs in diamond (simulated using SRIM²³). We also note that a standard anneal of the sample only creates a small fraction of the NV centers the SHIs created. After annealing the sample, we observe additional NV centers at the end-of-range of the ions where most of the vacancies are created. Therefore we conclude that although vacancies are needed for the NV formation, the availability of vacancies alone is not enough to create NV centers and that energy deposition due to electronic stopping or ion recoils plays also an important role in effectively creating NV centers.

We estimate the self-absorption of the emitted light by the NV centers by using an absorption cross section²⁴ of $\sigma = 2.8 \times 10^{-17} \text{ cm}^2$ and a density of $n = 1.76 \times 10^{19} \text{ cm}^{-3}$ (equivalent to 100 ppm and 100 % activation) and calculating the transmission $T = \exp[-l\sigma n]$, where l is the length of the photon path. This results in a transmission larger then 98 % at a depth of $40\mu\text{m}$. We therefore can ignore the effect of self-absorption.

The observed NV^- distribution does seem to follow the electronic energy loss of the SHI closely. A possible explanations could be that this is due to the role of secondary electrons (or delta-electrons) that can be formed in close collisions of SHI with target electrons. Electrons with energies up to 10 keV can be formed in collisions with 1 GeV gold ions, well below the threshold for vacancy formation of 120 keV.¹⁷ Electrons can contribute in several ways to creating NV centers, for example by heating

and locally annealing the volume around the SHI track. Detailed energy-loss and energy transport simulations²⁵ and further experiments are ongoing.

The primary effect of thermal annealing in the SHI irradiated regions of the diamond is a broadening of the intensity-depth distribution that is centered deeper within the sample. The PL signal due to NV⁻ centers within the non-irradiated area also increased marginally in comparison to the irradiated region. By considering the difference in intensity between the irradiated and non-irradiated spectra of Fig. 3d, we observe that the 800 °C anneal does not reproduce the effect of SHI radiation exposure. Specifically, the intensity of the NV⁻ peak is approximately 100 times higher in the irradiated region than in the non-irradiated-annealed region. Measurements of quantitative changes in NV⁻ population due to ion irradiation (with and without annealing) are still in progress.

SHI transverse diamond samples on almost straight lines, with effective interaction track diameters of a few nm radius¹⁰ and trajectory lengths of tens of microns. NV centers hence form along a quasi 1D chain. The apparent density of NV centers in SHI irradiated areas is about 50× higher than in non-irradiated regions. Their average spacing will be given by the concentration and distribution of the nitrogen (present mostly as P1 centers) following single crystal growth together with the NV-formation efficiency per SHI. Thermal annealing will broaden the distribution due to defect diffusion processes.¹⁴ 1D chains of NV centers from low fluence irradiations (e.g. 1×10^6 ions/cm²) can be isolated from bulk samples using common lift-out techniques see e.g. Chai *et al.*,²⁶ and they can then be integrated, for example, with microwave sources and magnetic fields for exploration of spin-photon qubits with nearest neighbor coupling along a percolation chain. From the increase of the SHI induced NV intensities compared to non-irradiated regions in our diamonds with 100 ppm nitrogen concentration we estimate a conversion efficiency of at least 10% of nitrogen to NV centers.¹⁴ Within this estimate, 1.1 GeV gold ions form NV centers with an average spacing of a few nm over a distance of over ten microns in a quasi 1D register with potentially over one thousand qubits. A high nitrogen background concentration stabilizes NV-center charge states but the nitrogen spin bath will also limit spin coherence times to a few micro seconds at room temperature.²⁷

ACKNOWLEDGMENTS

The work at LBL was supported by the Office of Science, Office of Fusion Energy Sciences, of the U.S. Department of Energy, and Laboratory Directed Research and Development (LDRD) funding from Berkeley Lab, provided by the Director, Office of Science, of the U.S. Department of Energy, work at the Molecular Foundry was supported by the Office of Science, Office of Basic En-

ergy Sciences, of the U.S. Department of Energy, under Contract No. DE-AC02-05CH11231. The ion irradiation at GSI are based on a UMAT experiment, which was performed at the M-branch of the UNILAC at the GSI Helmholtzzentrum für Schwerionenforschung, Darmstadt (Germany) in the frame of FAIR Phase-0. REL acknowledges support from the Academy of Finland under grant No. 265675 and Aalto University Centre for Quantum Engineering. MT acknowledges funding from the European Union's Horizon 2020 Research and Innovation program under Grant Agreement No 730871.

DATA AVAILABILITY

The data, analysis scripts, and simulation scripts are openly available on Zenodo at <https://doi.org/10.5281/zenodo.4018144>, reference number 28.

- ¹T. Schröder, S. L. Mouradian, J. Zheng, M. E. Trusheim, M. Walsh, E. H. Chen, L. Li, I. Bayn, and D. Englund, "Quantum nanophotonics in diamond [invited]," *J. Opt. Soc. Am. B*, **JOSAB 33**, B65–B83 (2016).
- ²S. Wehner, D. Elkouss, and R. Hanson, "Quantum internet: A vision for the road ahead," *Science* **362** (2018), 10.1126/science.aam9288.
- ³F. Dolde, I. Jakobi, B. Naydenov, N. Zhao, S. Pezzagna, C. Trautmann, J. Meijer, P. Neumann, F. Jelezko, and J. Wrachtrup, "Room-temperature entanglement between single defect spins in diamond," *Nat. Phys.* **9**, 139–143 (2013).
- ⁴P. Deák, B. Aradi, M. Kaviani, T. Frauenheim, and A. Gali, "Formation of NV centers in diamond: A theoretical study based on calculated transitions and migration of nitrogen and vacancy related defects," *Phys. Rev. B Condens. Matter* **89**, 075203 (2014).
- ⁵J. Meijer, B. Burchard, M. Domhan, C. Wittmann, T. Gaebel, I. Popa, F. Jelezko, and J. Wrachtrup, "Generation of single color centers by focused nitrogen implantation," *Appl. Phys. Lett.* **87**, 261909 (2005).
- ⁶J. Schwartz, S. Aloni, D. F. Ogletree, M. Tomut, M. Bender, D. Severin, C. Trautmann, I. W. Rangelow, and T. Schenkel, "Local formation of nitrogen-vacancy centers in diamond by swift heavy ions," *J. Appl. Phys.* **116**, 214107 (2014).
- ⁷D. M. Toyli, C. D. Weis, G. D. Fuchs, T. Schenkel, and D. D. Awschalom, "Chip-scale nanofabrication of single spins and spin arrays in diamond," *Nano Lett.* **10**, 3168–3172 (2010).
- ⁸M. Koenig, A. Benuzzi-Mounaix, A. Ravasio, T. Vinci, N. Ozaki, S. Lepape, D. Batani, G. Huser, T. Hall, D. Hicks, A. MacKinnon, P. Patel, H. S. Park, T. Boehly, M. Borghesi, S. Kar, and L. Romagnani, "Progress in the study of warm dense matter," *Plasma Physics and Controlled Fusion* **47**, B441–B449 (2005).
- ⁹D. Schwen, E. Bringa, J. Krauser, A. Weidinger, C. Trautmann, and H. Hofsäss, "Nano-hillock formation in diamond-like carbon induced by swift heavy projectiles in the electronic stopping regime: Experiments and atomistic simulations," *Appl. Phys. Lett.* **101**, 113115 (2012).
- ¹⁰D. Schwen and E. M. Bringa, "Atomistic simulations of swift ion tracks in diamond and graphite," *Nucl. Instrum. Methods Phys. Res. B* **256**, 187–192 (2007).
- ¹¹F. Valencia, J. D. Mella, R. I. González, M. Kiwi, and E. M. Bringa, "Confinement effects in irradiation of nanocrystalline diamond," *Carbon N. Y.* **93**, 458–464 (2015).
- ¹²F. C. Waldermann, P. Olivero, J. Nunn, K. Surmacz, Z. Y. Wang, D. Jaksch, R. A. Taylor, I. A. Walmsley, M. Draganski, P. Reichart, A. D. Greentree, D. N. Jamieson, and S. Praver, "Creating diamond color centers for quantum optical applications," *Diam. Relat. Mater.* **16**, 1887–1895 (2007).

- ¹³Z. Huang, W.-D. Li, C. Santori, V. M. Acosta, A. Faraon, T. Ishikawa, W. Wu, D. Winston, R. S. Williams, and R. G. Beausoleil, "Diamond nitrogen-vacancy centers created by scanning focused helium ion beam and annealing," *Appl. Phys. Lett.* **103**, 081906 (2013).
- ¹⁴V. M. Acosta, E. Bauch, M. P. Ledbetter, C. Santori, K.-M. C. Fu, P. E. Barclay, R. G. Beausoleil, H. Linget, J. F. Roch, F. Treussart, S. Chemerisov, W. Gawlik, and D. Budker, "Diamonds with a high density of nitrogen-vacancy centers for magnetometry applications," *Phys. Rev. B Condens. Matter* **80**, 115202 (2009).
- ¹⁵V. S. Varichenko, A. M. Zaitsev, and V. F. Stelmakh, "Luminescence of natural IIa diamond implanted with nitrogen ions," *phys. stat. sol. (a)* **95**, K25–K28 (1986).
- ¹⁶P. Racke, R. Wunderlich, J. W. Gerlach, J. Meijer, and D. Spemann, "Nanoscale ion implantation using focussed highly charged ions," *New J. Phys.* **22**, 083028 (2020).
- ¹⁷J. Schwartz, S. Aloni, D. F. Ogletree, and T. Schenkel, "Effects of low-energy electron irradiation on formation of nitrogen-vacancy centers in single-crystal diamond," *New J. Phys.* **14**, 043024 (2012).
- ¹⁸S. Pezzagna, B. Naydenov, F. Jelezko, J. Wrachtrup, and J. Meijer, "Creation efficiency of nitrogen-vacancy centres in diamond," *New J. Phys.* **12**, 065017 (2010).
- ¹⁹J. Botsoa, T. Sauvage, M.-P. Adam, P. Desgardin, E. Leoni, B. Courtois, F. Treussart, and M.-F. Barthe, "Optimal conditions for nV^- center formation in type-1b diamond studied using photoluminescence and positron annihilation spectroscopies," *Phys. Rev. B* **84**, 125209 (2011).
- ²⁰T. Luhmann, R. John, R. Wunderlich, J. Meijer, and S. Pezzagna, "Coulomb-driven single defect engineering for scalable qubits and spin sensors in diamond," *Nat. Commun.* **10**, 4956 (2019).
- ²¹E. S. Barnard, E. T. Hoke, S. T. Connor, J. R. Groves, T. Kuykendall, Z. Yan, E. C. Samulon, E. D. Bourret-Courchesne, S. Aloni, P. J. Schuck, C. H. Peters, and B. E. Hardin, "Probing carrier lifetimes in photovoltaic materials using subsurface two-photon microscopy," *Sci. Rep.* **3**, 2098 (2013).
- ²²N. J. Everall, "Confocal raman microscopy: Why the depth resolution and spatial accuracy can be much worse than you think," *Appl. Spectrosc.* **54**, 1515–1520 (2000).
- ²³J. F. Ziegler, M. D. Ziegler, and J. P. Biersack, "SRIM - The stopping and range of ions in matter (2010)," *Nuclear Instruments and Methods in Physics Research B* **268**, 1818–1823 (2010).
- ²⁴S. D. Subedi, V. V. Fedorov, J. Peppers, D. V. Martyshkin, S. B. Mirov, L. Shao, and M. Loncar, "Laser spectroscopic characterization of negatively charged nitrogen-vacancy (NV^-) centers in diamond," *Opt. Mater. Express, OME* **9**, 2076–2087 (2019).
- ²⁵J. J. Barnard and T. Schenkel, "Modeling of intense pulsed ion beam heated masked targets for extreme materials characterization," *J. Appl. Phys.* **122**, 195901 (2017).
- ²⁶G. Chai, H. Heinrich, L. Chow, and T. Schenkel, "Electron transport through single carbon nanotubes," *Appl. Phys. Lett.* **91**, 103101 (2007).
- ²⁷J. A. van Wyk, E. C. Reynhardt, G. L. High, and I. Kiflawi, "The dependences of ESR line widths and spin - spin relaxation times of single nitrogen defects on the concentration of nitrogen defects in diamond," *J. Phys. D Appl. Phys.* **30**, 1790 (1997).
- ²⁸R. E. Lake, M. Tomut, C. Trautmann, C. Christian, A. Persaud, E. S. Barnard, E. M. Chan, and T. Schenkel, "Data, analysis scripts, and simulations files for "depth profiles of the defects formed by swift heavy ions in diamond"," [10.5281/zenodo.4018144](https://zenodo.org/record/4018144) (2020), Zenodo.